

3-(Fur-2-yl)-10-(2-phenylethyl)-[1,2,4]triazino[4,3-*a*]benzimidazol-4(10*H*)-one, a Novel Adenosine Receptor Antagonist with A_{2A}-Mediated Neuroprotective Effects

Alessia Scatena,[†] Francesco Fornai,^{†,‡} Maria Letizia Trincavelli,^{||} Sabrina Taliani,[⊥] Simona Daniele,[§] Isabella Pugliesi,[⊥] Sandro Cosconati,[#] Claudia Martini,^{||} and Federico Da Settimo^{*,⊥}

[†]Dipartimento di Morfologia Umana e Biologia Applicata, Università di Pisa, Via Roma 55, 56126 Pisa, Italy

[‡]Neurobiologia dei disturbi del movimento, IRCCS INM Neuromed, Via Atinense 18, 86077 Pozzilli, Isernia, Italy

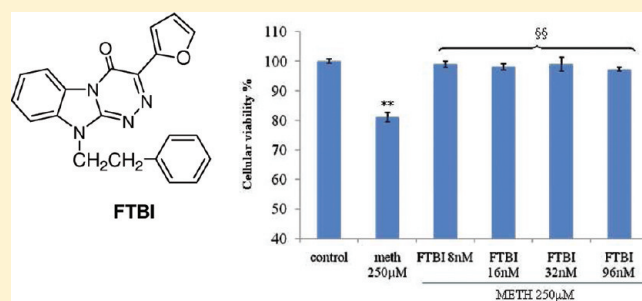
[§]Department of Drug Discovery and Development, Istituto Italiano di Tecnologia, via Morego, 30, 16163 Genova, Italy

^{||}Dipartimento di Psichiatria, Neurobiologia, Farmacologia e Biotecnologie, Università di Pisa, Via Bonanno 6, 56126 Pisa, Italy

[⊥]Dipartimento di Scienze Farmaceutiche, Università di Pisa, Via Bonanno 6, 56126 Pisa, Italy

[#]Dipartimento di Scienze Ambientali, Seconda Università di Napoli, Via Vivaldi 43, 81100 Caserta, Italy

ABSTRACT: In this study, compound FTBI (3-(2-furyl)-10-(2-phenylethyl)-[1,2,4]triazino[4,3-*a*]benzimidazol-4(10*H*)-one) was selected from a small library of triazinobenzimidazole derivatives as a potent A_{2A} adenosine receptor (AR) antagonist and tested for its neuroprotective effects against two different kinds of dopaminergic neurotoxins, 1-methyl-4-phenylpyridinium (MPP⁺) and methamphetamine (METH), in rat PC12 and in human neuroblastoma SH-SY5Y cell lines. FTBI, in a concentration range corresponding to its affinity for A_{2A} AR subtype, significantly increased the number of viable PC12 cells after their exposure to METH and, to a similar extent, to MPP⁺, as demonstrated in both trypan blue exclusion assay and in cytological staining. These neuroprotective effects were also observed with a classical A_{2A} AR antagonist, ZM241385, and appeared to be completely counteracted by the AR agonist, NECA, supporting A_{2A} ARs are directly involved in FTBI-mediated effects. Similarly, in human SH-SY5Y cells, FTBI was able to prevent cell toxicity induced by MPP⁺ and METH, showing that this A_{2A} AR antagonist has a neuroprotective effect independently by the specific cell model. Altogether these results demonstrate that the A_{2A} AR blockade mediates cell protection against neurotoxicity induced by dopaminergic neurotoxins in dopamine containing cells, supporting the potential use of A_{2A} AR antagonists in dopaminergic degenerative diseases including Parkinson's disease.



KEYWORDS: A_{2A} AR antagonists, neurotoxins, neuroprotection, PC12 cells, human neuroblastoma cells, cell viability

Adenosine is a physiological nucleoside which plays an important role in many patho-physiological conditions, at central and peripheral levels, through the modulation of specific membrane G-protein coupled receptors (GPCRs), currently classified into A₁, A_{2A}, A_{2B}, and A₃. Responses to activation of adenosine receptors (ARs) are mediated by different second messenger systems, such as adenylate cyclase, calcium or potassium channels (A₁ AR), phospholipase C (A₁, A_{2B}, and A₃ ARs), and phospholipase D (A₃ AR).^{1–4}

Each AR subtype is currently considered an attractive target for pharmacological intervention in many pathological conditions.^{5,6} Within the central nervous system (CNS), ARs possess a relevant role in the occurrence, development, and treatment of brain ischemic damage and degenerative disorders by modulating neuronal and synaptic functions. Particularly, it is now widely recognized that AR ligands may represent good candidates for the development of innovative therapeutic strategies for the treatment of the symptoms and progression of neurodegenerative diseases.^{7–11}

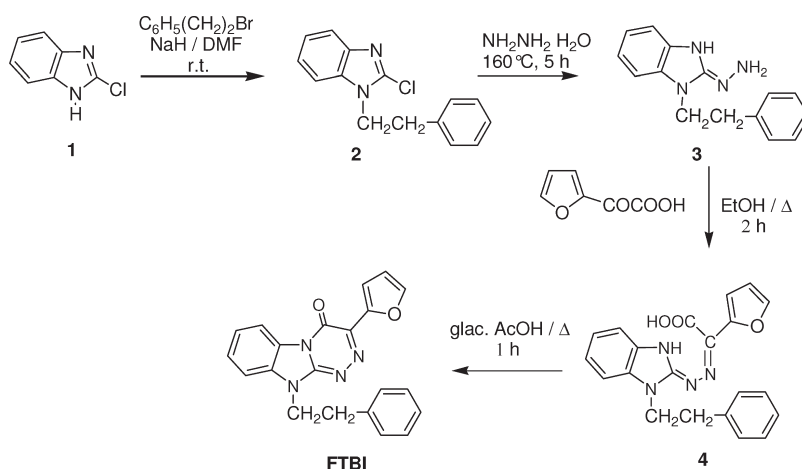
Differently from the widely recognized neuroprotective role exerted by A₁ AR, in the last years, A_{2A} AR has raised great interest in the medicinal chemistry community as it has proved to be an attractive target for therapeutic intervention in neurodegenerative movement disorders including Parkinson's¹² and Huntington's disease,¹³ dystonia such as restless leg syndrome, dyskinesia such as those caused by prolonged use of neuroleptic and dopaminergic drugs,¹⁴ as well as in ischemic damage. The protection from neuronal damage by A_{2A} ARs was first proposed by Gao and Phillis in a gerbil model of cerebral ischemia injury.¹⁵ Later on, it was confirmed that either the pharmacological receptor blockade with selective antagonists or the genetic elimination of A_{2A} ARs conferred a robust neuroprotection in animal models of brain ischemia.^{16,17} This was later extended against a variety of insults

Received: April 11, 2011

Accepted: June 10, 2011

Published: June 10, 2011

Scheme 1. Chemical Synthesis of FTBI



to adult brain tissue, such as glutamate excitotoxicity and free radical toxicity.^{18,19}

The neuroprotective effects of A_{2A} AR antagonists may reside in the blockade of A_{2A} AR-mediated glutamate release by astrocytes.²⁰ Specifically, during ischemia in the brain, the concentration of adenosine may rise to levels at which A_{2A} ARs are activated, increasing the release of the excitotoxic amino acid glutamate,²¹ which may induce or facilitate the occurrence of damage. Under these circumstances, A_{2A} AR antagonists are expected to counteract the increase in glutamate release and, in turn, to diminish the extent of neuronal damage, with few effects on other areas of the brain or peripheral tissues.²²

In dealing with specific neurodegenerative disorders, robust evidence bridges the protective effects of A_{2A} AR antagonists to Parkinson's disease. Such an effect may occur at two different levels: (i) protection of dopamine (DA)-containing neurons against cell death; (ii) prevention of the onset of behavioral sensitization leading to the occurrence of dyskinesia induced by DA replacement therapy. The latter effect is widely documented in relationship with the A_{2A} ARs modulation of dopamine receptors.^{23–25} This led to clinical trials with A_{2A} AR antagonists in Parkinson's disease with promising results.^{26,27} The neuroprotective effects of A_{2A} AR antagonists against DA cell death are supported by studies showing that these compounds protect nigral DA neurons from cell loss induced by the mitochondrial neurotoxin 1-methyl-4-phenyl-1,2,3,6-tetrahydropyridine (MPTP).²⁸ MPTP is converted into the toxic metabolite 1-methyl-4-phenylpyridinium (MPP⁺) which in turn is selectively taken up by DA-containing neurons where it produces cell death due to inhibition of mitochondrial respiratory chain.^{29,30}

The design, synthesis, and biological study of new AR ligands to obtain compounds endowed with enhanced activity and selectivity are an ongoing research project in our group. Over the past decade, we have disclosed numerous classes of selective A_1 AR antagonists^{31–34} and selective A_3 AR antagonists.^{34–37} With the aim to identify novel potent AR antagonists, the class of 3-aryl-[1,2,4]triazino[4,3-*a*]benzimidazol-4(10*H*)ones^{31,32} was further investigated. A small library of derivatives was synthesized and tested, permitting identification of compound FTBI, featuring a 2-phenylethyl group at the 10-position and a 2-furyl moiety at the 3-position of the triazinobenzimidazole nucleus, with a significant A_{2A} AR affinity (see Scheme 1). A number of pharmacokinetic properties, including the BBB permeability, were predicted in

silico for FTBI to support its potential use as a pharmacological agent acting at the SNC level. The results prompted us to characterize FTBI for its biological activity by means of "in vitro" studies. Specifically, FTBI was assayed for its binding properties for ARs and selectivity toward other receptors including GABA_A, glutamate NMDA, and D₂ dopamine receptor. In addition, its A_{2A} AR efficacy profile was assessed together with the ability to exert neuroprotective effects in two different types of DA-containing cells (i.e., PC12 and SH-SY5Y cells) and with two different kinds of DA neurotoxins bearing a different mechanism of action, MPP⁺ and methamphetamine (METH).

RESULTS AND DISCUSSION

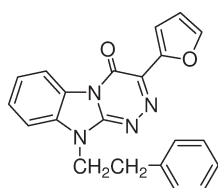
Chemical Synthesis. The synthetic pathway yielding the novel triazinobenzimidazole derivative FTBI is outlined in Scheme 1. It involves the synthesis of 2-chloro-1-(2-phenylethyl)benzimidazole **2** by alkylation of the commercially available 2-chlorobenzimidazole **1** with 2-bromoethylbenzene in the presence of sodium hydride.³⁸ Heating **2** with hydrazine hydrate at 180 °C in a Pyrex capped tube yielded the 2-hydrazone derivative **3**, that was allowed to react in refluxing ethanol with (furan-2-yl)oxoacetic acid for 2 h. In agreement with our previous findings,^{31,39} the obtaining of the target tricyclic compound FTBI proceeded through the formation of the intermediate 2-(benzimidazol-2-ylhydrazono)-2-furyl acetic acid **4** which was separated by cooling of the reaction mixture. It was isolated by filtration and purified by suspension in hot methanol. The final cyclization process was performed by refluxing the acid **4** for 1 h in glacial acetic acid.

In Silico Evaluation of the Pharmacokinetic Properties of FTBI. To achieve optimum therapeutic efficacy, our AR antagonist should possess a high degree of potency and selectivity toward the target as well the capability to cross the blood-brain barrier (BBB) to attain a certain concentration in the target tissue. Such a capability mostly depends on different physicochemical properties of the inspected compound. These features have been in silico calculated (Table 1) through the Qikprop program (Schrödinger, LLC, New York) to predict their propensity to cross the BBB and compared with those of a prototypical A_{2A} AR antagonist ZM241385.⁴⁰ As shown in Table 1, FTBI has a high probability of entering the CNS. In fact, all parameters fall in the requested ranges (molecular weight (MW) less than 450, ClogP less than 5, number of H-bond acceptors less than 7, polar surface area (PSA)

Table 1. Prediction of Some Pharmacokinetic Properties of FTBI

compd	MW ^a	donor HB ^b	accept HB ^c	ClogP ^d	QPP MDCK ^e	HOAP ^f	PSA ^g	rule of five ^h	RB ⁱ	ClogBB ^j
FTBI	356.3	0	5.5	3.7	1394.8	100	58.7	0	3	-0.185
ZM 241385	337.3	4	6.75	1.5	59.15	74	118.6	0	3	-1.72

^a Molecular weight. ^b Number of hydrogen bond donors. ^c Number of hydrogen bond acceptors; values are averages taken over a number of configurations, so they can be noninteger. ^d Calculated *n*-octanol/water partition coefficient. ^e Predicted apparent MDCK cell permeability in nm/s. MDCK cells are considered to be a good mimic for the blood-brain barrier (<25, poor; >500, great). ^f Predicted human oral absorption on 0–100% scale. ^g van der Waals surface area of polar nitrogen and oxygen atoms. ^h Number of violations of the Lipinsky's rule of five. ⁱ Number of rotatable bonds. ^j Predicted brain/blood partition coefficient (range of recommended values -3.0–1.2).

Table 2. Binding Affinities of FTBI to Different Membrane Receptors

compd	K_i (nM) ^a					
	hA ₁ ^b	hA _{2A} ^c	hA ₃ ^d	rGABA _A ^e	rNMDA ^f	hD ₂ ^g
FTBI	>10 000	16 ± 1.5	>1000	>10 000	>10 000	>10 000
DPCPX	0.5 ± 0.03	337 ± 28	>1000			
NECA	14 ± 4	16 ± 3	73 ± 5			
Cl-IBMECA	890 ± 61	401 ± 25	0.22 ± 0.02			

^a The K_i values are means ± SEM derived from an iterative curve-fitting procedure (Prism program, GraphPad, San Diego, CA). ^b Displacement of specific [³H]DPCPX binding in membranes obtained from hA₁ AR stably expressed in CHO cells. ^c Displacement of specific [³H]NECA binding in membranes obtained from hA_{2A} AR stably expressed in CHO cells. ^d Displacement of specific [¹²⁵I]AB-MECA binding in membranes obtained from hA₃ AR stably expressed in CHO cells. ^e Displacement of specific [³H]Ro151788 binding in membranes obtained from rat cerebral cortex. ^f Displacement of specific [³H]MK-801 binding in membranes obtained from rat cerebral cortex. ^g Displacement of specific [³H]YM09151-2 binding in membranes obtained from hD₂ DR stably expressed in CHO cells.

less than 90 Å, number of rotatable bonds (RB) less than or equal to 10), and, most of all, both the logBB and penetration potential of MDCK cells would indicate a good possibility to reach cerebral tissues.

Binding Receptor Affinity. FTBI was tested in radioligand binding assays to determine its affinity toward human A₁, A_{2A}, and A₃ ARs, by competition experiments assessing its respective ability to displace [³H]-8-cyclopentyl-1,3-dipropylxanthine [³H]DPCPX, [³H]-5'-(*N*-ethylcarboxamide)adenosine [³H]NECA, and [¹²⁵I]-N⁶-(3-iodo-4-aminobenzyl)-5'-*N*-methylcarboxamidoadenosine [¹²⁵I]AB-MECA binding from transfected CHO cells. Experiments were performed as described elsewhere.³² The affinity values of FTBI are reported in Table 2, together with the affinity data of DPCPX, NECA, and Cl-IBMECA taken as reference standards. FTBI displayed a high affinity toward A_{2A} AR, with a K_i value of 16 ± 1.5 nM, and complete selectivity versus A₁ and A₃ ARs. In addition, FTBI affinity toward other membrane receptors, including GABA_A, NMDA, and D₂ dopamine receptors, was evaluated. Results depicted in Table 2 show the compound was totally inactive to these receptors.

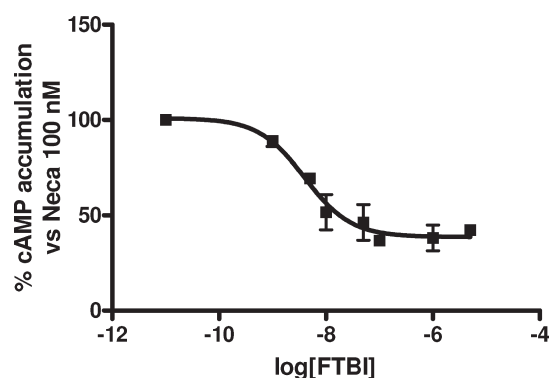


Figure 1. Effect of FTBI on NECA-stimulated cAMP accumulation in A_{2A} CHO cells. Cells were treated with 100 nM NECA in the absence or in the presence of different FTBI concentrations (1 nM to 10 μM). Then the intracellular levels of cAMP were evaluated and expressed as percentage of NECA-stimulated cAMP levels set to 100%. Data represent means ± SEM of three separate experiments each performed in duplicate.

FTBI was also tested in functional assays at human A_{2A} ARs by measuring its effects on NECA-mediated cAMP modulation in A_{2A} AR transfected CHO cells (Figure 1).⁴¹ FTBI displayed a full antagonism profile with a potency (IC₅₀ = 3.88 ± 0.85 nM, Figure 1) comparable to its binding affinity. Furthermore, when tested in the absence of NECA, it did not show any significant effect on the cAMP level even after stimulation by forskolin, thereby indicating the compound behaves as neutral antagonist (data not shown).

Neuroprotection Studies in PC12 and SH-SY5Y Cell Lines.

In order to evaluate the neuroprotective efficacy of FTBI, we used different types of DA-containing cells, the rat pheochromocytoma cell line (PC12) and the human neuroblastoma cell line (SH-SY5Y), and two different kinds of DA neurotoxins bearing different mechanisms of action, MPP+ and METH (see Methods). The former produces DA damage due to inhibition of complex I in mitochondrial respiratory chain,^{29,30} causing, in turn, cell death. This model is widely used to screen for potential neuroprotective effects in parkinsonism.^{28,42} The DA neurotoxin METH is able to determine a protein misfolding due to a massive DA release,^{43–46} and to produce DA cell death in vitro and loss of DA axons in vivo.^{47–49} METH also induces DA-dependent abnormal involuntary movements expressed as stereotypes when administered in vivo.⁵⁰ The use of two different cell lines and two different models of neurotoxicity allows one to probe and double-validate the neuroprotective effects of FTBI independently by cell- and toxin-specific effects.

Preliminarily, experiments were performed to evaluate the neurotoxic effects produced by MPP+ and METH on PC12 and

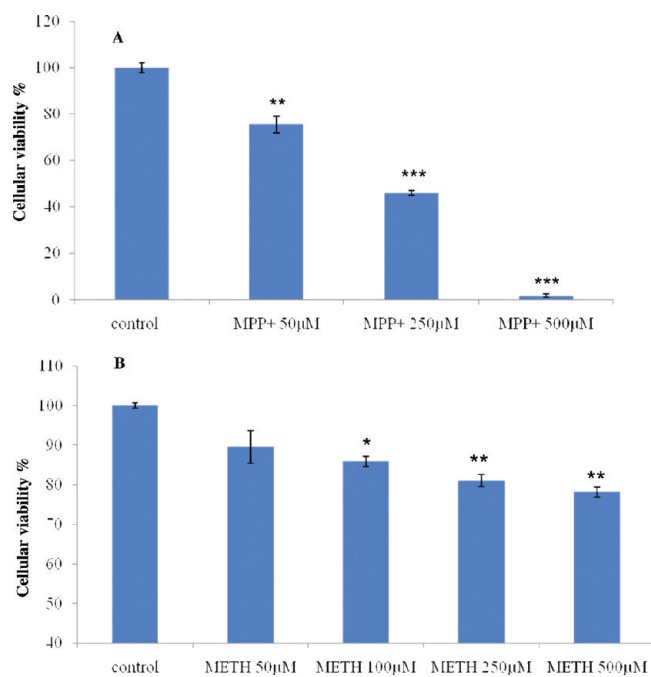


Figure 2. Dose-dependency of MPP⁺ (A) and METH (B) toxicity in PC12 cells. Cell counts were carried out following 72 h of MPP⁺ (A) or METH (B) exposure. Effects of DA toxins on cell viability were measured by using trypan blue staining. Results shown are expressed as means \pm SEM of at least four independent experiments. * P < 0.05 compared with control; ** P < 0.01 compared with control; *** P < 0.001 compared with control.

SH-SY5Y cells. In fact, especially METH toxicity considerably varies depending on the experimental setting; therefore, we specifically drew a dose–response curve in order to assess in the present experimental conditions the toxic doses of METH.

In pilot experiments, the neurotoxic effects of MPP⁺ in PC12 cells were evaluated by treating the cells with different neurotoxin concentrations ranging from 50 to 500 μ M. The results depicted in Figure 2A show that MPP⁺ produced a significant and concentration-dependent neurotoxic effect in this cell line. The percentage of cell viability was $2.00 \pm 0.16\%$ and $45.9 \pm 0.99\%$ after 72 h treatment with 500 and 250 μ M MPP⁺, respectively. The dose of 250 μ M, which caused an intermediate level of cell death, is optimal to detect both potential neuroprotective and/or neurotoxic effects of the new compound, and then it was chosen for the subsequent neuroprotection studies. The neurotoxic effects of METH, in the same cell line, were evaluated by incubating PC12 cells with different neurotoxin concentrations ranging from 50 to 500 μ M. In a similar way to MPP⁺, METH induced a concentration-dependent neurotoxic effect in PC12 cells (Figure 2B), and the concentration of 250 μ M was selected for the subsequent neuroprotection studies. The neurotoxic effects of this toxin appeared to be lower than that obtained with MPP⁺: the percentage of cell viability was $75.0 \pm 4.20\%$ after 72 h treatment with 500 μ M METH. The same neurotoxins, MPP⁺ and METH, showed neurotoxic effects also in SH-SY5Y cells, although at higher concentrations (1.5 and 2.5 mM, respectively; data not shown). The different neurotoxin doses required to obtain comparable neurotoxicity in the two different cell cultures reflects the cell-type-dependent vulnerability of DA-containing cells.⁴²

The compound FTBI, when administered alone, did not affect PC12 cell viability as demonstrated both in trypan blue exclusion

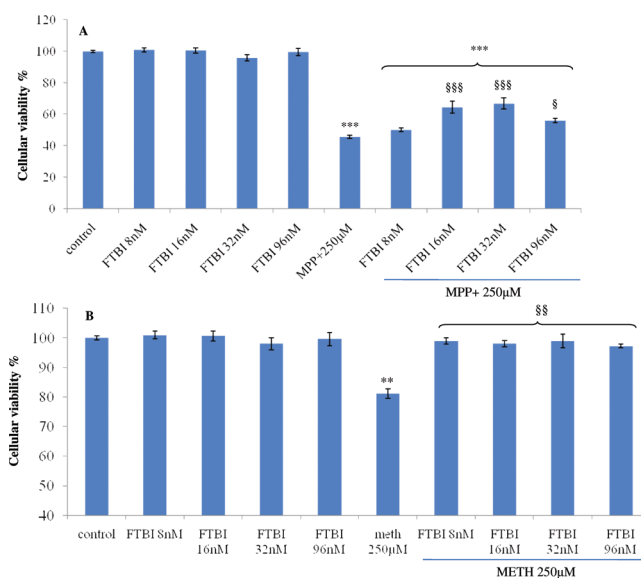


Figure 3. FTBI induced neuroprotection against MPP⁺ or METH toxicity. PC12 cells were treated for 72 h with 250 μ M MPP⁺ (A) or METH (B) in the absence or in the presence of different FTBI concentrations. Effects of different treatments on cell viability were measured by using trypan blue staining. Results shown are expressed as means \pm SEM of at least four independent experiments. *** P < 0.001 compared with control; § P < 0.05 compared with toxin alone; §§§ P < 0.001 compared with toxin alone.

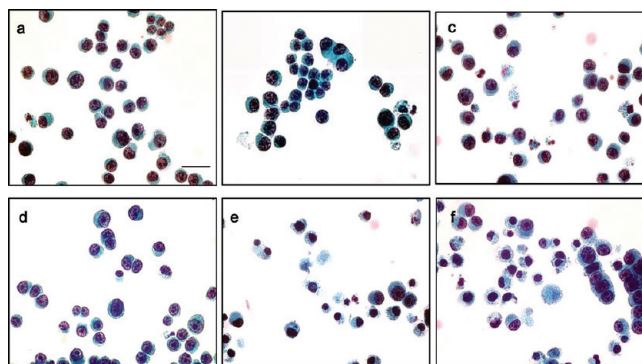


Figure 4. Representative pictures of protective effects of FTBI against METH and MPP⁺ toxicity: Papanicolaou's staining. PC12 cells were treated with either METH (250 μ M) or MPP⁺ (250 μ M), in the absence or in the presence of the adenosine antagonist FTBI (16 nM). (a) control; (b) FTBI (16 nM); (c) METH (250 μ M); (d) METH (250 μ M) plus FTBI (16 nM); (e) MPP⁺ (250 μ M); (f) MPP⁺ (250 μ M) plus FTBI (16 nM). Scale bar: 12.5 μ m.

assay (Figure 3) and in cytological staining (Figure 4). FTBI, in a concentration range between 16 and 96 nM, was able to partially counteract MPP⁺-induced neurotoxicity (Figure 3A), although this effect did not appear to be concentration-dependent. FTBI was also able to protect PC12 cells from METH-induced neurotoxicity with similar efficacy (Figure 3B): following cell treatment with FTBI at the lowest concentration tested of 8 nM, the cell viability appeared to be completely restored up to the level of control untreated cells. These results demonstrated that FTBI was similarly effective in protecting cells from METH- or MPP⁺-induced neurotoxicity.

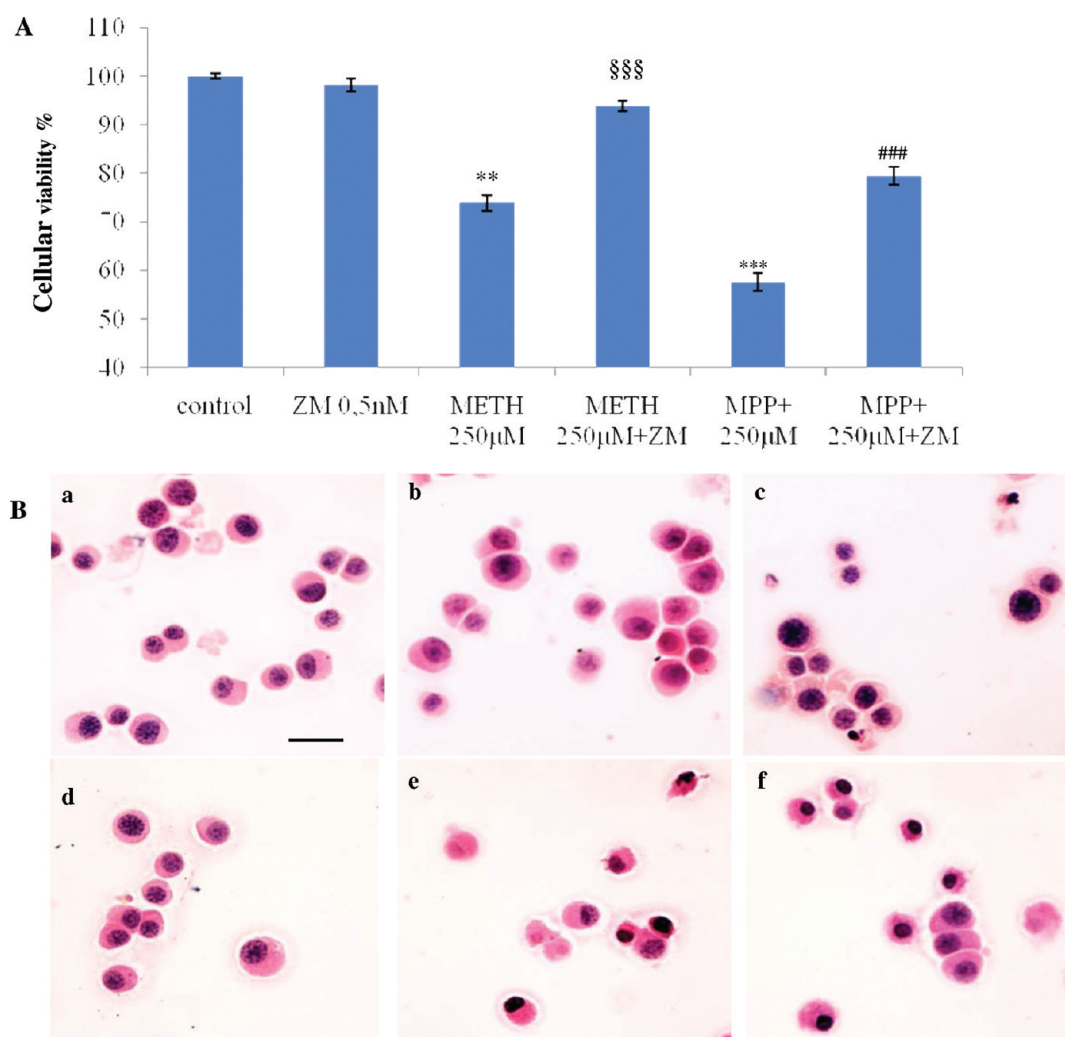


Figure 5. ZM241385-induced neuroprotection against METH or MPP⁺ toxicity. PC12 cells were treated for 72 h with 250 μ M METH or MPP⁺ in the absence or in the presence of 0.5 nM ZM241385. Effects of different treatments on cell viability were measured by using trypan blue (A) and H&E (B) staining. Results in (A) are expressed as means \pm SEM of at least four independent experiments. ** P < 0.01 compared with control; *** P < 0.001 compared with control; §§§ P < 0.001 compared with METH (250 μ M); ### P < 0.001 compared with MPP⁺ alone. (B) Representative pictures of the protective effects of ZM241385 (a) control; (b) ZM241385 (0.5 nM); (c) METH (250 μ M); (d) METH (250 μ M) plus ZM241385 (0.5 nM); (e) MPP⁺ (250 μ M); (f) MPP⁺ (250 μ M) plus ZM241385 (0.5 nM). Scale bar: 8.3 μ m.

As shown in representative pictures obtained with Papanicolaou's staining, spared cells appear shrunken with pyknotic nuclei (Figure 4). Cell morphology was altered in the METH treated group (panel c). Cell pretreatment with FTBI preserved the morphology of the cell culture (panel d) that appeared similar to that of cells in the control group (panel a). When the cells were treated with MPP⁺, their morphology was severely altered (panel e), while they were partially preserved by pretreatment with FTBI (panel f). The data obtained in cytological experiments are in line with those obtained in cell viability assay, confirming that FTBI displays a similar neuroprotective effect in METH- and MPP⁺-induced damage.

As stated above, FTBI is a potent A_{2A} AR antagonist with no effect on other relevant central receptors, such as GABA_A, glutamate NMDA, and D₂ dopamine. However, in order to verify that the neuroprotective effects exerted by FTBI were really ascribable to the selective block of A_{2A} ARs, (i) we compared the effects of the compound with those of a prototypical A_{2A} AR antagonist, ZM241385, and (ii) we evaluated whether the FTBI-mediated effects were counteracted by the AR agonist NECA.

As shown in Figure 5A, the A_{2A} AR antagonist ZM241385, used at a concentration corresponding to its IC₅₀ value toward A_{2A} AR subtype, displayed a neuroprotective effect on PC12 cells counteracting METH- and MPP⁺-induced toxicity to a similar extent. The antagonist alone did not affect PC12 cell viability. These results demonstrate that the selective block of A_{2A} AR subtypes significantly protects PC12 cells by death induced by different kinds of DA toxicity. Representative histochemistry analysis (hematoxylin and eosin (H&E) staining) showed PC12 morphological changes in line with data obtained with trypan blue exclusion assay (Figure 5B).

To validate the involvement of A_{2A} AR in the neuroprotective effects of FTBI against METH toxicity, we evaluated the ability of the AR agonist, NECA, to reverse FTBI effects. PC12 cells were treated with FTBI (32 nM) either in the absence or in the presence of three different NECA concentrations ranging from 50 to 200 nM. Results depicted in Figure 6 show that the agonist NECA abolished the protective effects of FTBI in METH-treated cells, thus confirming that the effects of FTBI are likely ascribable to the

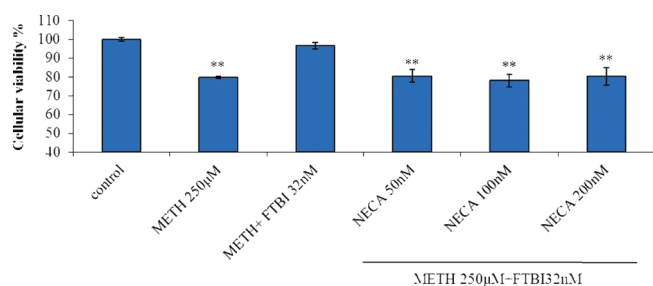


Figure 6. Neuroprotection induced by the A_{2A} antagonist FTBI is lost by the coadministration of the adenosine agonist NECA. PC12 cells were treated for 72 h with 250 μ M METH in the absence and in the presence of 32 nM FTBI and different concentrations of NECA ranging from 50 to 200 nM. Effects of different treatments on cell viability were measured by using trypan blue staining. Results shown are expressed as means \pm SEM of at least four independent experiments. ** $P < 0.01$ compared with control.

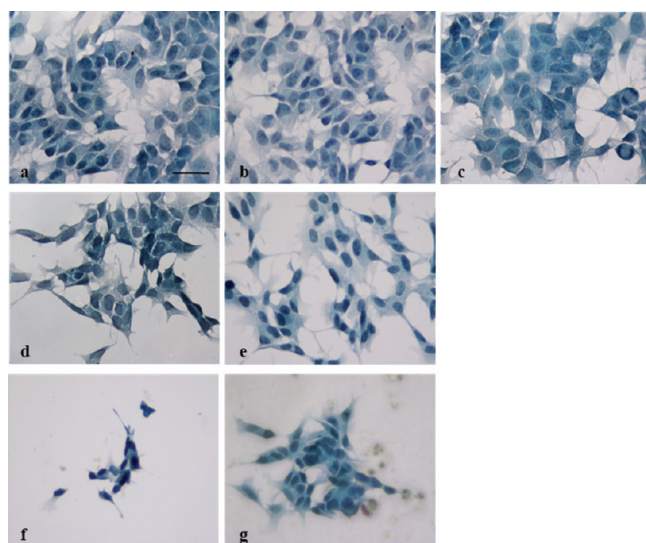


Figure 7. Representative pictures of protective effects of FTBI against METH and MPP+ toxicity in SH-SY5Y cells. SH-SY5Y cells were treated with either METH (2.5 mM) or MPP+ (1.5 mM) in the absence and in the presence of FTBI (16 and 32 nM). These pictures are representative of numerical data matching those obtained in PC12 cells. (a) Control; (b) FTBI (16 nM); (c) FTBI (32 nM); (d) METH (2.5 mM); (e) METH (2.5 mM) plus FTBI (16 nM); (f) MPP+ (1.5 mM); (g) MPP+ (1.5 mM) plus FTBI (32 nM). Scale bar: 40 μ m.

selective block of A_{2A} ARs. In fact, although NECA is a nonselective agonist for all AR subtypes, PC12 cells mainly express this AR subtype, allowing one to speculate that this receptor is the target protein for FTBI.

Again, when we sought to validate our findings in SH-SY5Y cells, which represents an *in vitro* model of neuronal cells more adherent to DA neurons, FTBI did not affect per se the number of living cells, while it was able to prevent to a similar extent the toxicity induced by METH or MPP+ (Figure 7). Protection was obtained using the same doses of FTBI (16 nM and 32 nM) as in the test with PC12 cells.

CONCLUSIONS

As part of an ongoing research project of our group, the class of 3-aryl[1,2,4]triazino[4,3-*a*]benzimidazol-4(10*H*)ones was further

investigated with the aim to identify novel potent AR antagonists. For this purpose, a small library of derivatives was synthesized and tested, permitting identification of the compound FTBI, featuring a 2-phenylethyl group at the 10-position and a 2-furyl moiety at the 3-position of the triazinobenzimidazole nucleus, which showed a significant A_{2A} AR affinity and *in silico* pharmacokinetic properties consistent with the ability to cross the BBB. In functional assays at human A_{2A} ARs, FTBI displayed a profile of full neutral antagonism with a potency comparable to its binding affinity. Furthermore, FTBI did not show any affinity toward other relevant membrane receptors, such as GABA_A, NMDA, and D₂ dopamine receptors.

Two different types of DA-containing cells (i.e., PC12 and SH-SY5Y cells) and two different kinds of DA neurotoxins (i.e., METH and MPP+) were employed to assess the ability of FTBI to exert neuroprotective effects. Actually, FTBI, at concentrations comparable to its affinity toward A_{2A} AR subtypes, proved to be able to similarly prevent (20–25%) toxicity induced by METH and MPP+ in both cell lines. In PC12 cells, a prototypical A_{2A} AR antagonist ZM241385 (0.5 nM) exerted a similar protective effect as that displayed by FTBI against both DA neurotoxins, and the AR agonist NECA counteracted FTBI effects against METH toxicity. Taken together, the above results suggest that the neuroprotective effects of FTBI depend on A_{2A} ARs antagonism and occur independently of cell line and experimental model. The inactivation of A_{2A} AR might then play a key role in the protection mechanism against neurotoxicity induced by DA neurotoxins in DA-containing cells.

Finally, it has to be pointed out that this is the first report in which the beneficial effect of A_{2A} AR antagonists against METH-induced, DA-dependent cell death has been disclosed. Such an effect supports the potential use of A_{2A} AR antagonists in dopaminergic neurodegenerative diseases, including Parkinson's disease, and fosters a novel therapeutic application of these molecules in drug abuse.

METHODS

Chemistry. Synthesis of FTBI (3-(Fur-2-yl)-10-(2-phenylethyl)-[1,2,4]triazino[4,3-*a*]benzimidazol-4(10*H*)-one). Melting points were determined using a Reichert Köfeler hot-stage apparatus and are uncorrected. Infrared spectra were recorded with a Nicolet/Avatar FT-IR spectrometer in Nujol mulls. Routine nuclear magnetic resonance spectra were recorded in DMSO-*d*₆ solution on a Varian Gemini 200 spectrometer operating at 200 MHz. Evaporation was performed *in vacuo* (rotary evaporator). Analytical TLC was carried out on Merck 0.2 mm precoated silica gel aluminum sheets (60 F-254). Combustion analyses on target compounds were performed by our Analytical Laboratory in Pisa. All compounds showed $\geq 95\%$ purity.

2-Chlorobenzimidazole 1, 2-phenylethyl bromide, α -oxo-2-furanacetic acid, reagents, and solvents were from Sigma-Aldrich. The 2-chloro-1-(2-phenylethyl)benzimidazole 2 was prepared in accordance with a reported procedure.³⁸

1-(2-Phenylethyl)-1,3-dihydro-2*H*-benzimidazol-2-one Hydrazone 3. 2-Chloro-1-(2-phenylethyl)benzimidazole 2 (0.692 g, 2.7 mmol) was heated at 180 °C in a Pyrex capped tube with 1.0 mL of hydrazine monohydrate for 5 h. After the mixture was cooled, a white solid separated, which was collected and was sufficiently pure to be used in the next reaction without further purification. Yield: 92%; mp = 99–101 °C. IR (nujol, cm^{-1}): 3500–2650, 1620, 1600, 1560, 1140, 740. ¹H NMR (DMSO-*d*₆, ppm): 3.12 (t, 2H, $J = 7.1$ Hz), 4.50 (t, 2H, $J = 7.3$ Hz), 7.03–7.46 (m, 7H), 7.62 (dd, 2H, $J = 7.6, 1.0$ Hz). Anal. Calcd. for

C₁₅H₁₆N₄ (%): C, 71.40; H, 6.39; N, 22.21. Found: C, 71.17; H, 6.45; N, 22.36.

{[1-(2-Phenylethyl)-1,3-dihydro-2H-benzimidazol-2-ylidene]hydrazono}(2-furyl)acetic Acid **4**. A solution of 1-(2-phenylethyl)-1,3-dihydro-2H-benzimidazol-2-one hydrazone **3** (1.01 g, 4 mmol) and 2-furyl-oxoacetic acid (0.616 g, 4.4 mmol) in 10 mL of absolute ethanol was refluxed for 2 h. After cooling, the precipitate which formed was collected to give (benzimidazol-2-ylhydrazono)acetic acid **4** which was purified by suspension in hot methanol. Yield: 65%; mp = 202–204 °C. IR (nujol, cm⁻¹): 3200–2800, 1650, 1620, 1280, 1140, 740. ¹H NMR (DMSO-*d*₆, ppm): 3.06 (t, 2H, *J* = 7.5 Hz), 4.29 (t, 2H, *J* = 7.6 Hz), 6.61 (dd, 1H, *J* = 3.3, 1.9 Hz), 7.16–7.49 (m, 10H); 7.78 (dd, 1H, *J* = 1.0, 0.5 Hz), 12.34 (bs, 1H). Anal. Calcd. for C₂₁H₁₈N₄O₃ (%): C, 67.37; H, 4.85; N, 14.96. Found: C, 67.23; H, 4.91; N, 15.07.

3-(2-Furyl)-10-(2-phenylethyl)[1,2,4]triazino[4,3-*a*]benzimidazol-4(10H)-one **FTBI**. A suspension of {[1-(2-phenylethyl)-1,3-dihydro-2H-benzimidazol-2-ylidene]hydrazono}(2-furyl)acetic acid **4** (0.748 g, 2 mmol) in 20 mL of glacial acetic acid was refluxed for 1 h. The solution obtained was evaporated to dryness, and the oily residue was purified by recrystallization from ethanol. Yield: 62%; mp = 190–192 °C. IR (nujol, cm⁻¹): 1675, 1560, 1480, 1150, 750. ¹H NMR (DMSO-*d*₆, ppm): 3.19 (t, 2H, *J* = 7.3 Hz), 4.65 (t, 2H, *J* = 7.3 Hz), 6.70 (dd, 1H, *J* = 1.4, 0.6 Hz), 7.17–7.67 (m, 9H), 7.91 (dd, 1H, *J* = 0.8, 0.6 Hz), 8.47 (dd, 1H, *J* = 8.0, 0.6 Hz). Anal. Calcd. for C₂₁H₁₆N₄O₂ (%): C, 70.77; H, 4.53; N, 15.72. Found: C, 70.48; H, 4.60; N, 15.59.

Receptor Binding Assay. Human Adenosine Receptors. CHO cells stably expressing human A₁, A_{2A}, and A₃ ARs were kindly supplied by Prof. K. N. Klotz, Wurzburg University, Germany.⁵¹

Human A₁ Adenosine Receptors. Aliquots of membranes (30 μg proteins) obtained from A₁ CHO cells were incubated at 25 °C for 180 min in 500 μL of T₁ buffer (50 mM Tris-HCl, 2 mM MgCl₂, 2 units/mL ADA, pH 7.4) containing [³H]DPCPX (3 nM) and six different concentrations of the newly synthesized compound. Nonspecific binding was determined in the presence of 50 μM R-PIA.³² The dissociation constant (*K_d*) of [³H]DPCPX in A₁ CHO cell membranes was 3 nM.

Human A_{2A} Adenosine Receptors. Aliquots of cell membranes (20 μg proteins) were incubated at 25 °C for 180 min in 500 μL of T₂ buffer (50 mM Tris-HCl, 2 mM MgCl₂, 2 units/mL ADA, pH 7.4) in the presence of 30 nM of [³H]NECA and six different concentrations of the newly synthesized compound. Nonspecific binding was determined in the presence of 100 μM NECA.³² The dissociation constant (*K_d*) of [³H]NECA in A_{2A} CHO cell membranes was 30 nM.

Human A₃ Adenosine Receptors. Aliquots of cell membranes (40 μg proteins) were incubated at 25 °C for 90 min in 100 μL of T₃ buffer (50 mM Tris-HCl, 10 mM MgCl₂, 1 mM EDTA, 2 units/mL ADA, pH 7.4) in the presence of 1.4 nM [¹²⁵I]ABMECA and six different concentrations of the newly synthesized compound. Nonspecific binding was determined in the presence of 50 μM R-PIA.³² The dissociation constant (*K_d*) of [¹²⁵I]AB-MECA in A₃ CHO cell membranes was 1.4 nM.

GABA_A Receptors. The affinity of FTBI to GABA_A receptors was evaluated by incubating aliquots of rat brain membranes (50 μg) at 0 °C for 90 min in 500 μL buffer (50 mM Tris citrate pH 7.4) in the presence of 0.2 nM [³H]Ro151788 and different compound concentrations (100 nM, 10 μM). Nonspecific binding was estimated in the presence of 10 μM diazepam.⁵²

NMDA Receptors. The affinity of FTBI to NMDA glutamate receptors was evaluated by incubating aliquots of rat brain membranes (50 μg) at 23 °C for 60 min in 1 mL buffer (4.5, HEPES 5 mM, pH 7.4) in the presence of 3 nM [³H]MK-801 and different compound concentrations (100 nM, 10 μM). Nonspecific binding was determined in the presence of unlabeled (1)-MK-801 100 μM.⁵³

D₂ Dopamine Receptors. The affinity of FTBI to D₂ DR was evaluated by incubating aliquots of CHO cell membranes (30 μg) at 30 °C for

60 min in 1 mL of binding buffer (50 mM Tris-HCl, 155 mM NaCl, pH 7.4, 1.5 mM ascorbic acid) in the presence of 0.05 nM [³H]YM09151-2 and different compound concentrations (100 nM, 10 μM). Nonspecific binding was determined in the presence of 1.5 mM dopamine.⁵⁴

FTBI was routinely dissolved in dimethyl sulfoxide (DMSO) and diluted with assay buffer to the final concentration, where the amount of DMSO never exceeded 2%. Percentage inhibition values of specific radiolabeled ligand binding at 1–10 μM concentration are means ± SEM of at least three determinations. At least six different concentrations spanning 3 orders of magnitude, adjusted appropriately for the IC₅₀ of the compound, were used. IC₅₀ values, computer-generated using a nonlinear regression formula on a computer program (GraphPad, San Diego, CA), were converted to *K_i* values, knowing the *K_d* values of radioligand in the different tissues and using the Cheng and Prusoff equation.⁵⁵ *K_i* values are means ± SEM of at least three determinations.

Measurement of Cyclic AMP Levels in hA_{2A} CHO Cells. Intracellular cyclic AMP (cAMP) levels were measured using a competitive protein binding method.⁴¹ CHO cells, expressing recombinant human A_{2A} ARs, were harvested by trypsinization. After centrifugation and resuspension in medium, cells (~60 000) were plated in 24-well plates in 0.5 mL of medium. After 48 h, the medium was removed, and the cells were incubated at 37 °C for 15 min with 0.5 mL of Dulbecco's modified Eagle's medium (DMEM) in the presence of Ro20-1724 (20 μM), as phosphodiesterase inhibitor, and adenosine deaminase (1 U/mL). The antagonistic profile of the new compound toward A_{2A} AR was evaluated assessing its ability to counteract 100 nM NECA-mediated stimulation of cAMP. Cells were incubated in the reaction medium (15 min at 37 °C) with different compound concentrations (1 nM to 10 μM) and then treated with NECA. In parallel, aliquots of cells were treated with the compound alone (10 μM) in the absence or in the presence of forskolin. The reaction was terminated by the removal of the medium and the addition of 0.4 N HCl. After 30 min, lysates were neutralized with 4 N KOH, and the suspension was centrifuged at 800g for 5 min. For determination of cAMP production, cAMP binding protein, isolated from beef adrenal glands, was incubated with [³H]cAMP (2 nM), 50 μL of cell lysate, or cAMP standard (0–16 pmol) at 0 °C for 150 min in a total volume of 300 μL. Bound radioactivity was separated by rapid filtration through GF/C glass fiber filters and washed twice with 4 mL of 50 mM Tris/HCl pH 7.4. The radioactivity was measured by liquid scintillation spectrometry.

Neuroprotection Studies. The neuroprotective effects of the compound FTBI were evaluated in PC12 and SH-SY5Y cells following induction of cell death by two different DA neurotoxins: MPP+ or METH.

PC12 Cell. The PC12 cell line was obtained from the American Type Culture Collection (ATCC) and grown in RPMI 1640 medium supplemented with heat-inactivated 10% horse serum (HS) and 5% fetal bovine serum (FBS), including penicillin (50 IU/mL) and streptomycin (50 mg/mL). Cells were grown in 75 cm² tissue culture flasks and maintained in a humidified atmosphere of 5% carbon dioxide (CO₂) at 37 °C. The medium was changed every 3 days and maintained at the conditions described above. Cells were used for the experiments when they were in log-phase.

SH-SY5Y Cell. The SH-SY5Y cell line was obtained from the ATCC and grown in RPMI 1640 medium supplemented with 10% FBS, including penicillin (50 IU/mL) and streptomycin (50 mg/mL). Cells were maintained in a humidified atmosphere of 5% CO₂ at 37 °C. The medium was changed every 3 days and maintained at the conditions described above.

Cell Treatments. PC12 cells were seeded in 6-well plates at 5 × 10⁵ cells in a final volume of 1.5 mL/well. SH-SY5Y cells were seeded in a Chamber Slide system with 8 wells on glass (C7182, Sigma Nunc Lab-Tek) at 3 × 10⁴ cells in a final volume of 500 μL/well. Cells were incubated at 37 °C in 5% CO₂ for 72 h in the presence of MPP+ or METH at different concentrations ranging from 50 to 500 μM. The doses of

both toxins producing a significant neurotoxic effect were determined (250 μ M MPP+ and METH for PC12 cells and 1.5 mM MPP+ and 2.5 mM METH for SH-SY5Y cells) and used in the following neuroprotection experiments.

For neuroprotection experiments, cells were treated for 72 h with MPP+ or METH in the presence of different FTBI concentrations (8–96 nM), selected on the basis of compound affinity calculated in binding studies. In parallel, to evaluate whether the FTBI neuroprotective effects were likely ascribed to the selective block of A_{2A} AR subtypes, aliquots of PC12 cells were treated with (i) the antagonist ZM241385 (0.5 nM) or with (ii) the agonist NECA (500–200 nM) in the presence of 32 nM FTBI.

At the end of the cell treatments, cells were processed in various ways: (1) For light microscopy, they were centrifuged and the pellets were dissolved in buffer, applied on glass slides by cytospin (12 000g \times 10 min), and processed for Papanicolaou's staining or H&E staining. (2) For assessment of cytotoxicity, an aliquot of cells was collected, diluted in a solution containing trypan blue, and counted. SH-SY5Y cells were directly stained on the chamber slide.

MPP+ and METH solutions were prepared by dissolving the powder in culture medium RPMI. A_{2A} AR antagonist and agonist solutions were prepared by dissolving the powder in culture medium RPMI and adding DMSO at a concentration of less than 1%.

Cell Viability Assay by Colloidal Dye (Trypan Blue) Exclusion. Healthy living cells contain plasma membranes that effectively exclude most large hydrophilic molecules. However, injured cells with compromised membrane integrity can allow hydrophilic molecules, such as trypan blue, into their cytoplasm. This assay is based on the simple principle that viable cells will exclude the trypan blue dye, whereas dead or dying neurons will not, thus appearing blue. Live and/or dead cells are incubated with the dye and then counted in situ using bright field optics with a grid-containing eyepiece. Cell viability was expressed as number of viable cells/total cell number and indicated as percent survival compared to the corresponding controls (untreated cells). The viability of control cells was defined as 100%.

Papanicolaou's and H&E Staining. The morphological changes associated with the death of PC12 and SH-SY5Y cells induced by treatment were also detected by cytological staining according to the Papanicolaou method⁵⁶ or H&E method.

Data Analysis. Comparisons among groups were made by using a one-way ANOVA using Scheffé post hoc tests. Null hypothesis was rejected for $P < 0.05$.

AUTHOR INFORMATION

Corresponding Author

*Mailing address: Department of Pharmaceutical Sciences, University of Pisa, Via Bonanno 6, 56126 Pisa, Italy. Telephone: (+39-050) 2219561. Fax: (+39-050) 2219605. E-mail: fsettimo@farm.unipi.it.

Funding Sources

This work was financially supported by MIUR (PRIN 2008).

Author Contributions

A.S. carried out the experiments for the neuroprotection studies and elaborated results. F.F. designed the protocols for the neuroprotection studies and played a fundamental role as supervisor of the experiments; he elaborated results and contributed to the discussion of the results and to writing the article. M.L.T. designed the protocols for the evaluation of FTBI affinity and pharmacological profile, also playing a fundamental role as supervisor of the experiments; she elaborated results and contributed to the discussion of the results and to writing the article. S.T. designed the protocols for the synthesis of FTBI, also

playing a fundamental role as supervisor of the experiments; she also contributed to writing the manuscript. S.D. carried out the experiments for the evaluation of FTBI affinity and pharmacological profile and elaborated results. I.P. synthesized FTBI and performed its structural characterization. S.C. performed in silico evaluation of the pharmacokinetic properties of FTBI; he elaborated results and contributed to writing the article. C.M. gave a fundamental contribution to the significance of the results, and provided important help with writing the article discussion section. F.D.S. coordinated the research project, gave a fundamental contribution to the significance of the results, and provided important help with writing the article discussion section. All authors contributed to and have approved the final manuscript.

ACKNOWLEDGMENT

We thank Prof. Dr. Karl-Norbert Klotz for his generous gift of transfected CHO cells expressing human A₁, A_{2A}, and A₃ receptors.

ABBREVIATIONS

AR, adenosine receptor; BBB, blood-brain barrier; CNS, central nervous system; DA, dopamine; [³H]DPCPX, [³H]-8-cyclopentyl-1,3-dipropylxanthine; GPCRs, G-protein coupled receptors; [¹²⁵I]AB-MECA, [¹²⁵I]-N⁶-(3-iodo-4-aminobenzyl)-5'-N-methyl-carboxamidoadenosine; METH, methamphetamine; MPP+, 1-methyl-4-phenylpyridinium; MPTP, 1-methyl-4-phenyl-1,2,3,6-tetrahydropyridine; [³H]NECA, [³H]-5'-(N-ethylcarboxamide)adenosine; PBS, phosphate-buffered saline

REFERENCES

- (1) Poulsen, S. A., and Quinn, R. J. (1998) Adenosine receptors: new opportunities for future drugs. *Bioorg. Med. Chem.* 6, 619–641.
- (2) Fredholm, B. B., Arslan, G., Halldner, L., Kull, B., Schulte, G., and Wasserman, W. (2000) Structure and function of adenosine receptors and their genes. *Naunyn-Schmiedeberg's Arch. Pharmacol.* 362, 364–374.
- (3) Fredholm, B. B., IJzerman, A. P., Jacobson, K. A., Klotz, K.-N., and Linden, J. (2001) International Union of Pharmacology. XXV. Nomenclature and classification of adenosine receptors. *Pharmacol. Rev.* 53, 527–552.
- (4) Schulte, G., and Fredholm, B. B. (2000) Human adenosine A(1), A(2A), A(2B), and A(3) receptors expressed in Chinese hamster ovary cells all mediate the phosphorylation of extracellular-regulated kinase 1/2. *Mol. Pharmacol.* 58, 477–482.
- (5) Jacobson, K. A., and Gao, Z. G. (2006) Adenosine receptors as therapeutic targets. *Nat. Rev. Drug Discovery* 5, 247–264.
- (6) Moro, S., Gao, Z. G., Jacobson, K. A., and Spalluto, G. (2006) Progress in the pursuit of therapeutic adenosine receptor antagonists. *Med. Res. Rev.* 26, 131–159.
- (7) Ribeiro, J. A., Sebastiao, A. M., and de Mendonca, A. (2002) Adenosine receptors in the nervous system: pathophysiological implications. *Prog. Neurobiol.* 68, 377–392.
- (8) Muller, C. E. (1997) A1-adenosine receptor antagonists. *Expert Opin. Ther. Pat.* 7, 419–440.
- (9) Muller, C. E. (2000) A2A-adenosine receptor antagonists-future drugs for Parkinson's disease?. *Drugs Future* 25, 1043–1052.
- (10) Baraldi, P. G., Tabrizi, M. A., Gessi, S., and Borea, P. A. (2008) Adenosine receptor antagonists: translating medicinal chemistry and pharmacology into clinical utility. *Chem. Rev.* 108, 238–263.
- (11) Press, N. J., Gessi, S., Borea, P. A., and Polosa, R. (2007) Therapeutic potential of adenosine receptor antagonists and agonists. *Expert Opin. Ther. Pat.* 17, 979–991.
- (12) Morelli, M., Carta, A. R., and Jenner, P. (2009) Adenosine A2A receptors and Parkinson's disease. *Handb. Exp. Pharmacol.* 193, 589–615.

- (13) Popoli, P., Blum, D., Domenici, M. R., Burnouf, S., and Chern, Y. (2008) A critical evaluation of adenosine A2A receptors as potentially "druggable" targets in Huntington's disease. *Curr. Pharm. Des.* 14, 1500–1511.
- (14) Trevitt, J., Vallance, C., Harris, A., and Goode, T. (2009) Adenosine antagonists reverse the cataleptic effects of haloperidol: implications for the treatment of Parkinson's disease. *Pharmacol. Biochem. Behav.* 92, 521–527.
- (15) Gao, Y., and Phillis, J. W. (1994) CGS 15943, an adenosine receptor antagonist, reduces cerebral ischemic injury in the Mongolian gerbil. *Life Sci.* 55, 61–65.
- (16) Monopoli, A. L. G., Forlani, A., Mattavelli, A., and Ongini, E. (1998) Blockade of adenosine A2A receptors by SCH 58261 results in neuroprotective effects in cerebral ischemia in rats. *NeuroReport* 9, 3955–3959.
- (17) Chen, J. F., Huang, Z., Ma, J., Zhu, J., Moratalla, R., Standaert, D., Moskowitz, M. A., Fink, J. S., and Schwarzschild, M. A. (1999) A(2A) adenosine receptor deficiency attenuates brain injury induced by transient focal ischemia in mice. *J. Neurosci.* 19, 9192–9200.
- (18) Chen, J. F., Sonsalla, P. K., Pedata, F., Melani, A., Domenici, M. R., Popoli, P., Geiger, J., Lopes, L. V., and de Mendonca, A. (2007) Adenosine A2A receptors and brain injury: broad spectrum of neuroprotection, multifaceted actions and "fine tuning" modulation. *Prog. Neurobiol.* 83, 310–331.
- (19) Cuhna, R. A. (2005) Neuroprotection by adenosine in the brain: from A1 receptor activation to A2A receptor blockade. *Purinergic Signalling* 1, 111–134.
- (20) Pintor, A., Galluzzo, M., Grieco, R., Pezzola, A., Reggio, R., and Popoli, P. (2004) Adenosine A2A receptor antagonists prevent the increase in striatal glutamate levels induced by glutamate uptake inhibitors. *J. Neurochem.* 89, 152–6.
- (21) Popoli, P., Betto, P., Reggio, R., and Ricciarello, G. (1995) Adenosine A2A receptor stimulation enhances striatal extracellular glutamate levels in rats. *Eur. J. Pharmacol.* 287, 215–217.
- (22) Stone, T. W., Ceruti, S., and Abbracchio, M. P. (2009) Adenosine receptors and neurological disease: neuroprotection and neurodegeneration. *Handb. Exp. Pharmacol.* 193, 535–587.
- (23) Mally, J., and Stone, T. W. (1994) The effect of theophylline on parkinsonian symptoms. *J. Pharm. Pharmacol.* 46, 515–517.
- (24) Mally, J., and Stone, T. W. (1996) Potential role of adenosine antagonist therapy in pathological tremor disorders. *Pharmacol. Ther.* 72, 243–250.
- (25) Mally, J., and Stone, T. W. (1998) Potential role of adenosine A2A receptor antagonists in the treatment of movement disorders. *CNS Drugs* 10, 311–320.
- (26) Kanda, T., Jackson, M. J., Smith, L. A., Pearce, R. K., Nakamura, J., Kase, H., Kuwana, Y., and Jenner, P. (1998) Adenosine A2A antagonist: a novel antiparkinsonian agent that does not provoke dyskinesia in parkinsonian monkeys. *Ann. Neurol.* 43, 507–513.
- (27) Grondin, R., Bedard, P. J., Hadj Tahar, A., Gregoire, L., Mori, A., and Kase, H. (1999) Antiparkinsonian effect of a new selective adenosine A2A receptor antagonist in MPTP-treated monkeys. *Neurol.* 52, 1673–1677.
- (28) Ikeda, K., Kurokawa, M., Aoyama, S., and Kuwana, Y. (2002) Neuroprotection by adenosine A2A receptor blockade in experimental models of Parkinson's disease. *J. Neurochem.* 80, 262–270.
- (29) Nicklas, W. J., Vyas, I., and Heikkila, R. E. (1985) Inhibition of NADH-linked oxidation in brain mitochondria by 1-methyl-4-phenylpyridine, a metabolite of the neurotoxin, 1-methyl-4-phenyl-1,2,5,6-tetrahydropyridine. *Life Sci.* 36, 2503–2538.
- (30) Ramsay, R. R., Salach, J. I., and Singer, T. P. (1986) Inhibition of mitochondrial NADH dehydrogenase by pyridine derivatives and its possible relation to experimental and idiopathic parkinsonism. *Biochem. Biophys. Res. Commun.* 134, 743–748.
- (31) Da Settimo, F., Primofiore, G., Taliani, S., Marini, A. M., La Motta, C., Novellino, E., Greco, G., Lavecchia, A., Trincavelli, L., and Martini, C. (2001) 3-Aryl[1,2,4]triazino[4,3-*a*]benzimidazol-4(10H)-ones: a new class of selective A1 adenosine receptor antagonists. *J. Med. Chem.* 44, 316–327.
- (32) Da Settimo, F., Primofiore, G., Taliani, S., La Motta, C., Novellino, E., Greco, G., Lavecchia, A., Cosimelli, B., Iadanza, M., Klotz, K.-N., Tuscano, D., Trincavelli, M. L., and Martini, C. (2004) A1 adenosine receptor antagonists, 3-aryl[1,2,4]triazino[4,3-*a*]benzimidazol-4(10H)-ones (ATBIs) and *N*-alkyl and *N*-acyl-(7-substituted-2-phenylimidazo[1,2-*a*][1,3,5]triazin-4-yl)amines (ITAs): Different recognition of bovine and human binding sites. *Drug Dev. Res.* 63, 1–7.
- (33) Novellino, E., Abignente, E., Cosimelli, B., Greco, G., Iadanza, M., Laneri, S., Lavecchia, A., Rimoli, M. G., Da Settimo, F., Primofiore, G., Tuscano, D., Trincavelli, L., and Martini, C. (2002) Design, synthesis and biological evaluation of novel *N*-alkyl- and *N*-acyl-(7-substituted-2-phenylimidazo[1,2-*a*][1,3,5]triazin-4-yl)amines (ITAs) as novel A(1) adenosine receptor antagonists. *J. Med. Chem.* 45, 5030–5036.
- (34) Novellino, E., Cosimelli, B., Ehlardo, M., Greco, G., Iadanza, M., Lavecchia, A., Rimoli, M. G., Sala, A., Da Settimo, A., Primofiore, G., Da Settimo, F., Taliani, S., La Motta, C., Klotz, K.-N., Tuscano, D., Trincavelli, M. L., and Martini, C. (2005) 2-(Benzimidazol-2-yl)quinoxalines: a novel class of selective antagonists at human A(1) and A(3) adenosine receptors designed by 3D database searching. *J. Med. Chem.* 48, 8253–8260.
- (35) Da Settimo, F., Primofiore, G., Taliani, S., Marini, A. M., La Motta, C., Simorini, F., Salerno, S., Sergianni, V., Tuccinardi, T., Martinelli, A., Cosimelli, B., Greco, G., Novellino, E., Ciampi, O., Trincavelli, M. L., and Martini, C. (2007) 5-amino-2-phenyl[1,2,3]-triazolo[1,2-*a*][1,2,4]benzotriazin-1-one: a versatile scaffold to obtain potent and selective A3 adenosine receptor antagonists. *J. Med. Chem.* 50, 5676–5684.
- (36) Cosimelli, B., Greco, G., Ehlardo, M., Novellino, E., Da Settimo, F., Taliani, S., La Motta, C., Bellandi, M., Tuccinardi, T., Martinelli, A., Ciampi, O., Trincavelli, M. L., and Martini, C. (2008) Derivatives of 4-amino-6-hydroxy-2-mercaptopyrimidine as novel, potent, and selective A3 adenosine receptor antagonists. *J. Med. Chem.* 51, 1764–1770.
- (37) Taliani, S., La Motta, C., Mugnaini, L., Simorini, F., Salerno, S., Marini, A. M., Da Settimo, F., Cosconati, S., Cosimelli, B., Greco, G., Limongelli, V., Marinelli, L., Novellino, E., Ciampi, O., Daniele, S., Trincavelli, M. L., and Martini, C. (2010) Novel N2-substituted pyrazolo[3,4-*d*]pyrimidine adenosine A3 receptor antagonists: inhibition of A3-mediated human glioblastoma cell proliferation. *J. Med. Chem.* 53, 3954–3963.
- (38) Parihar, H. S., Suryanarayanan, A., Ma, C., Joshi, P., Venkataraman, P., Schulte, M. K., and Kirschbaum, K. S. (2001) 5-HT(3)R binding of lerisetron: an interdisciplinary approach to drug-receptor interactions. *Bioorg. Med. Chem. Lett.* 11, 2133–2136.
- (39) Primofiore, G., Da Settimo, F., Taliani, S., Marini, A. M., La Motta, C., Novellino, E., Greco, G., Gesi, M., Trincavelli, L., and Martini, C. (2000) 3-Aryl-[1,2,4]triazino[4,3-*a*]benzimidazol-4(10H)-ones: tricyclic heteroaromatic derivatives as a new class of benzodiazepine receptor ligands. *J. Med. Chem.* 43, 96–102.
- (40) Poucher, S. M., Keddie, J. R., Singh, P., Stogdall, S. M., Caulkett, P. W., Jones, G., and Coll, M. G. (1995) The in vitro pharmacology of ZM 241385, a potent, non-xanthine A2a selective adenosine receptor antagonist. *Br. J. Pharmacol.* 115, 1096–1102.
- (41) Nordstedt, C., and Fredholm, B. B. (1990) A modification of a protein-binding method for rapid quantification of cAMP in cell-culture supernatants and body fluid. *Anal. Biochem.* 189, 231–234.
- (42) Fornai, F., Lenzi, P., Lazzeri, G., Ferrucci, M., Fulceri, F., Giorgi, F. S., Falleni, A., Ruggieri, S., and Paparelli, A. (2007) Fine ultrastructure and biochemistry of PC12 cells: a comparative approach to understand neurotoxicity. *Brain Res.* 1129, 174–190.
- (43) Seiden, L. S. (1985) Methamphetamine: toxicity to dopaminergic neurons. *NIDA Res. Monogr.* 62, 100–116.
- (44) Fornai, F., Lenzi, P., Gesi, M., Soldani, P., Ferrucci, M., Lazzeri, G., Capobianco, L., Battaglia, G., De Blasi, A., Nicoletti, F., and Paparelli, A. (2004) Methamphetamine produces neuronal inclusions in the nigrostriatal system and in PC12 cells. *J. Neurochem.* 88, 114–123.
- (45) Gluck, M. R., Moy, L. Y., Jayatilke, E., Hogan, K. A., Manzano, L., and Sonsalla, P. K. (2001) Parallel increases in lipid and protein oxidative markers in several mouse brain regions after methamphetamine treatment. *J. Neurochem.* 79, 152–160.

(46) Fornai, F., Lenzi, P., Ferrucci, M., Lazzeri, G., di Poggio, A. B., Natale, G., Busceti, C. L., Biagioni, F., Giusiani, M., Ruggieri, S., and Paparelli, A. (2005) Occurrence of neuronal inclusions combined with increased nigral expression of alpha-synuclein within dopaminergic neurons following treatment with amphetamine derivatives in mice. *Brain Res. Bull.* 65, 405–413.

(47) Iacovelli, L., Fulceri, F., De Blasi, A., Nicoletti, F., Ruggieri, S., and Fornai, F. (2006) The neurotoxicity of amphetamines: bridging drugs of abuse and neurodegenerative disorders. *Exp. Neurol.* 201, 24–31.

(48) Ferrucci, M., Pasquali, L., Paparelli, A., Ruggieri, S., and Fornai, F. (2008) Pathways of methamphetamine toxicity. *Ann. N.Y. Acad. Sci.* 1139, 177–185.

(49) Ferrucci, M., Pasquali, L., Ruggieri, S., Paparelli, A., and Fornai, F. (2008) Alpha-synuclein and autophagy as common steps in neurodegeneration. *Parkinsonism Relat. Disord.* 14 (Suppl 2), S180–184.

(50) Seiden, L. S., Sabol, K. E., and Ricaurte, G. A. (1993) Amphetamine: effects on catecholamine systems and behavior. *Annu. Rev. Pharmacol. Toxicol.* 33, 639–677.

(51) Klotz, K.-N., Hessling, J., Hegler, J., Owman, C., Kull, B., Fredholm, B. B., and Lohse, M. J. (1998) Comparative pharmacology of human adenosine receptor subtypes - characterization of stably transfected receptors in CHO cells. *Naunyn-Schmiedeberg's Arch. Pharmacol.* 357, 1–9.

(52) Costanzo, A., Guerrini, G., Ciciani, G., Bruni, F., Selleri, S., Costa, B., Martini, C., Lucacchini, A., Aiello, P. M., and Ipponi, A. (1999) Benzodiazepine receptor ligands. 4. Synthesis and pharmacological evaluation of 3-heteroaryl-8-chloropyrazolo[5,1-c][1,2,4] benzotriazine 5-oxides. *J. Med. Chem.* 42 (12), 2218–2226.

(53) Trincavelli, M. L., Cuboni, S., Catena Dell'osso, M., Maggio, R., Klotz, K. N., Novi, F., Panighini, A., Daniele, S., and Martini, C. (2010) Receptor crosstalk: haloperidol treatment enhances A(2A) adenosine receptor functioning in a transfected cell model. *Purinergic Signalling* 6 (4), 373–381.

(54) Marvizón, J. C., Lewin, A. H., and Skolnick, P. (1989) 1-Aminocyclopropane carboxylic acid: a potent and selective ligand for the glycine modulatory site of the N-methyl-D-aspartate receptor complex. *J. Neurochem.* 52 (3), 992–994.

(55) Cheng, Y., and Prusoff, W. H. (1973) Relationship between the inhibition constant (K_i) and the concentration of inhibitor which causes 50% inhibition (I₅₀) of an enzymatic reaction. *Biochem. Pharmacol.* 22, 3099–3108.

(56) Papanicolau, G. N. (1942) A new procedure for staining vaginal smears. *Science* 95, 438–439.